

## Research paper

# Differential glucose and beta-hydroxybutyrate metabolism confers an intrinsic neuroprotection to the immature brain in a rat model of neonatal hypoxia ischemia

F.K. Odorcyk<sup>a,\*</sup>, L.E. Duran-Carabali<sup>a</sup>, D.S. Rocha<sup>a</sup>, E.F. Sanches<sup>d</sup>, A.P. Martini<sup>b</sup>, G.T. Venturin<sup>c</sup>, S. Greggio<sup>c</sup>, J.C. da Costa<sup>c</sup>, L.C. Kucharski<sup>a</sup>, E.R. Zimmer<sup>d,e,f</sup>, C.A. Netto<sup>a,b,d,g</sup>

<sup>a</sup> Graduate Program in Physiology, Universidade Federal do Rio Grande do Sul (UFRGS), Porto Alegre, RS, Brazil

<sup>b</sup> Graduate Program in Neuroscience, Universidade Federal do Rio Grande do Sul (UFRGS), Porto Alegre, RS, Brazil

<sup>c</sup> Preclinical Research Center, Brain Institute (Brains) of Rio Grande do Sul, Pontifical Catholic University of Rio Grande do Sul (PUCRS), Porto Alegre, Brazil

<sup>d</sup> Graduate Program in Biochemistry, Universidade Federal do Rio Grande do Sul (UFRGS), Porto Alegre, RS, Brazil

<sup>e</sup> Graduate Program in Pharmacology and therapeutics, Universidade Federal do Rio Grande do Sul (UFRGS), Porto Alegre, RS, Brazil

<sup>f</sup> Department of Pharmacology, Universidade Federal do Rio Grande do Sul (UFRGS), Porto Alegre, RS, Brazil

<sup>g</sup> Department of Biochemistry, Universidade Federal do Rio Grande do Sul (UFRGS), Porto Alegre, RS, Brazil

## ARTICLE INFO

## Keywords:

Neonatal hypoxia ischemia  
Brain metabolism  
[<sup>18</sup>F]FDG microPET  
Beta-hydroxybutyrate  
Brain development

## ABSTRACT

Neonatal hypoxia ischemia (HI) is the main cause of newborn mortality and morbidity. Preclinical studies have shown that the immature rat brain is more resilient to HI injury, suggesting innate mechanisms of neuroprotection. During neonatal period brain metabolism experience changes that might greatly affect the outcome of HI injury. Therefore, the aim of the present study was to investigate how changes in brain metabolism interfere with HI outcome in different stages of CNS development. For this purpose, animals were divided into 6 groups: HIP3, HIP7 and HIP11 (HI performed at postnatal days 3, 7 and 11, respectively), and their respective shams. *In vivo* [<sup>18</sup>F]FDG micro positron emission tomography (microPET) imaging was performed 24 and 72 h after HI, as well as *ex-vivo* assessments of glucose and beta-hydroxybutyrate (BHB) oxidation. At adulthood behavioral tests and histology were performed. Behavioral and histological analysis showed greater impairments in HIP11 animals, while HIP3 rats were not affected. Changes in [<sup>18</sup>F]FDG metabolism were found only in the lesion area of HIP11, where a substantial hypometabolism was detected. Furthermore, [<sup>18</sup>F]FDG hypometabolism predicted impaired cognition and worst histological outcomes at adulthood. Finally, substrate oxidation assessments showed that glucose oxidation remained unaltered and higher level of BHB oxidation found in P3 animals, suggesting a more resilient metabolism. Overall, present results show [<sup>18</sup>F]FDG microPET predicts long-term injury outcome and suggests that higher BHB utilization is one of the mechanisms that confer the intrinsic neuroprotection to the immature brain and should be explored as a therapeutic target for treatment of HI.

## 1. Introduction

Neonatal hypoxia ischemia (HI) is one of the main cause of mortality and morbidity in newborns (Perlman, 2004; Volpe, 2009). The surviving infants develop various degrees of neurologic deficits that range from slight cognitive impairments to severe cases of cerebral palsy (Volpe, 2009). This pathology affects both preterm and term newborns. Although the nature of the injury is similar (e.g. hypoxia and ischemia), the consequences and therapeutic interventions may present substantial differences according to the stage of brain maturation

(Jacobs et al., 2013).

The Rice-Vannucci rat model is one of the most widely used to mimic HI in pre-clinical settings. It combines the unilateral permanent occlusion of the common carotid artery with a period of hypoxic exposure. The age of induction of the HI model may vary according to the degree of brain development and, in order to model HI in very preterm infants (ranging from 28 to 32 weeks of gestation) the injury procedure is performed at post-natal day 3 (PND3) in rats (Alexander et al., 2014; Sanches et al., 2015; Sizonenko et al., 2005). In order to model the injury in late preterm newborns (32–36 weeks of gestation) the

\* Corresponding author at: Post-graduation Program of Physiology, Instituto de Ciências Básicas da Saúde (ICBS), Universidade Federal do Rio Grande do Sul (UFRGS), Rua Ramiro Barcelos 2600, anexo, CEP 90035-003 Porto Alegre, RS, Brazil.

E-mail address: [felipe.odorcyk@gmail.com](mailto:felipe.odorcyk@gmail.com) (F.K. Odorcyk).

<https://doi.org/10.1016/j.expneurol.2020.113317>

Received 5 February 2020; Received in revised form 8 April 2020

Available online 15 April 2020

0014-4886/ © 2020 Elsevier Inc. All rights reserved.

procedure is performed at PND7, and for modeling HI occurred in term infants (> 36 weeks of gestation) the procedure is performed at PND10 or 11 (Semple et al., 2013). Nevertheless, it is important to point out that which rat PND resembles exactly which phase of brain development in humans is still an issue of debate (Patel et al., 2014, 2015).

Previous studies have compared the differences of the same HI model induced at PND3 (HIP3) and at PND7 (HIP7) (Alexander et al., 2014; Sanches et al., 2015). They showed that the same insult, that caused impairments in spatial and aversive memory, in motor learning as well as significant reductions in striatum, cortex and hippocampus when HI was performed at P7, barely caused any detectable deficits when performed at P3 (Alexander et al., 2014; Sanches et al., 2015). The fact that HIP7 animals present lesions that are more severe than the same insult in HIP3 animals suggests the existence of an “intrinsic protection” of the brain in earlier stages of development. However, the mechanisms underlying this protection of the immature brain are not fully understood. Brain metabolism is likely to be among the features that may underlie the greater resilience of the immature brain to injury. It is well known that the immature brain uses around half of the glucose that the mature brain does in relation to its size, whereas it uses much higher levels of ketone bodies than the mature brain (Brekke et al., 2015). These differences seem to play a major role in HI outcome, while hyperglycemia is linked to detrimental outcome in clinical (Pinchefsky et al., 2019) and experimental HI studies (Park et al., 2001), administration of exogenous beta-hydroxybutyrate improves neuropathological score as well as reduces HI-induced cell death in rats (Lee et al., 2018). However, the capacity of brain cells to utilize either glucose or ketone bodies is also poorly understood in context of neonatal HI.

Brain metabolism has a predictive value in HI in humans (Zou et al., 2018). In fact, the severity of brain damage is crucial for determining the therapeutic approaches, since treatments such as hypothermia do not present the same beneficial effects in all injury severities (Chiang et al., 2017; Jacobs et al., 2013). In this context, [<sup>18</sup>F]FDG microPET has showed strong correlations with HI outcome in the clinical setting, being a useful tool to aid clinicians in choosing the best therapeutic approach for each case (Shi et al., 2012; Thorngren-Jerneck et al., 2001). Nevertheless, it is not known if these clinical findings are translated into the experimental settings, since the predictive value of [<sup>18</sup>F]FDG microPET scan neuroimaging in the first days after the induction of the HI model in rats has never been studied. The assessment of the replicability of clinical findings in the pre-clinical setting, this “back-translation” enables the usage of advanced methods of analysis, only possible in animal models with high translational value (Parent et al., 2017).

Therefore, the present study aims to investigate the different responses triggered by HI insult in brain metabolism, such as *in vivo* glucose metabolism and whether the utilization of glucose as well as ketone bodies are mechanisms underlying the immature brain “intrinsic protection” to HI injury. The better understanding of such mechanisms may assist in the search for therapeutic strategies to reduce the mortality and detrimental effects of infants suffering from HI.

## 2. Methodology

### 2.1. Animals

Adult female Wistar rats and their male pups were used in this study. Mating was planned so that all groups would have the appropriate age so that the HI procedure would be performed in the same day, meaning that there was at least one litter of each age used in this study in each HI induction procedure. Such litters were composed of an adult female and 10 male rat pups, in order to avoid the litter effect, each litter contained pups of at least 3 different mothers, with a maximum of 4 pups of the same mother in each litter. All litters were standardized at PND1. All experimental procedures were performed in accordance with the recommendations of the Council for International

Organizations of Medical Sciences (CIOMS - Publication 85–23, 1985) and the Brazilian Society of Science in Laboratory Animals - Law n° 11.794. Ethical approval was obtained by the review board of the Universidade Federal do Rio Grande do Sul protocol # 31632. Rats were housed in standard conditions in cages measuring 16 × 41 × 34 cm (height x width x length), provided with wood shaving bedding.

### 2.2. Neonatal hypoxia-ischemia

PND3, PND7 and PND11 male pups were randomly assigned for receiving either Sham or HI procedure. HI animals were anesthetized (isoflurane 4–5% for induction and 1.5–2% for maintenance) and underwent permanent right common carotid artery occlusion, as previously described (Sanches et al., 2013). Animals were kept in warming pads (37 °C) for 10 min to recover from anesthesia and were returned to the dam. Two hours after surgery, pups were placed in a hypoxia chamber with fraction inspired of oxygen (FIO<sub>2</sub>: 0.08) at 37 °C for 90 min. Sham animals underwent carotid artery isolation without occlusion and were kept under atmospheric conditions (FIO<sub>2</sub>: 0.21). At the end of hypoxic period, all pups returned to their dams.

### 2.3. Experimental design

Animals were divided into 6 groups, sham (Sh) and hypoxia ischemia (HI) operated in the PND3 (ShP3 and HIP3 respectively), in the PND7 (ShP7 and HIP7 respectively) and in the PND11 (ShP11 and HIP11 respectively). In surgery days litters of 10 male pups with a mother were randomly divided into Sham or HI groups. For every surgery day, at least one litter of each age was present. In Experiment I, 24 and 72 h after the surgery animals were submitted to microPET scan imaging. Animals were weaned at PND23 and behavioral tests were performed from PND60 onwards. After, animals underwent perfusion and brains were used for histological analysis. In Experiment II, animals of the same experimental groups were used for <sup>14</sup>C-Hydroxybutyric acid and <sup>14</sup>C-glucose incorporation into <sup>14</sup>CO<sub>2</sub> at 24 and 72 h after the injury.

#### 2.3.1. [<sup>18</sup>F]FDG microPET scan

MicroPET scans were conducted at the Preclinical Research Center of the Brain Institute of Rio Grande do Sul (BraIns). Brain microPET images were acquired 24 and 72 h post-HI. The animals were anesthetized individually using a mixture of isoflurane and oxygen (3–4% induction and 2–3% maintenance), and 250 µCi of [<sup>18</sup>F]FDG was administered intraperitoneally (Dagnino et al., 2019). The animals were returned to the home cage for a 40-min period of conscious tracer uptake and were placed on a heat plate to maintain the body temperature at 36 ± 1 °C. After the uptake period, the rats were placed in headfirst prone position on the heated bed of the equipment (Triumph microPET, LabPET-4, TriFoil Imaging, Northridge, CA, USA). The static acquisition was performed under inhalational anesthesia for 10 min with the field of view (FOV: 3.75 cm) centered on the head (Nunes Azevedo et al., 2020; Zanirati et al., 2018).

#### 2.3.2. Image reconstruction and data analysis

An exploratory analysis of glucose metabolism was performed in the whole brain, cortex, striatum, hippocampus and corpus callosum bilaterally. All images were reconstructed using a 3-dimensional maximum likelihood expectation maximization (3D-MLEM) algorithm with 20 iterations (Zanirati et al., 2018). MicroPET images were manually co-registered to a standard magnetic resonance imaging (MRI) histological templates corresponding to animals age. MRI templates were obtained from the Duke Center for *In Vivo* Microscopy NIBIB P41 EB015897 (Calabrese et al., 2013). Standard uptake values (SUVs) were calculated using the following equation: SUV = (radioactivity)/(dose injected/body weight). Each hemisphere SUV was calculated based on

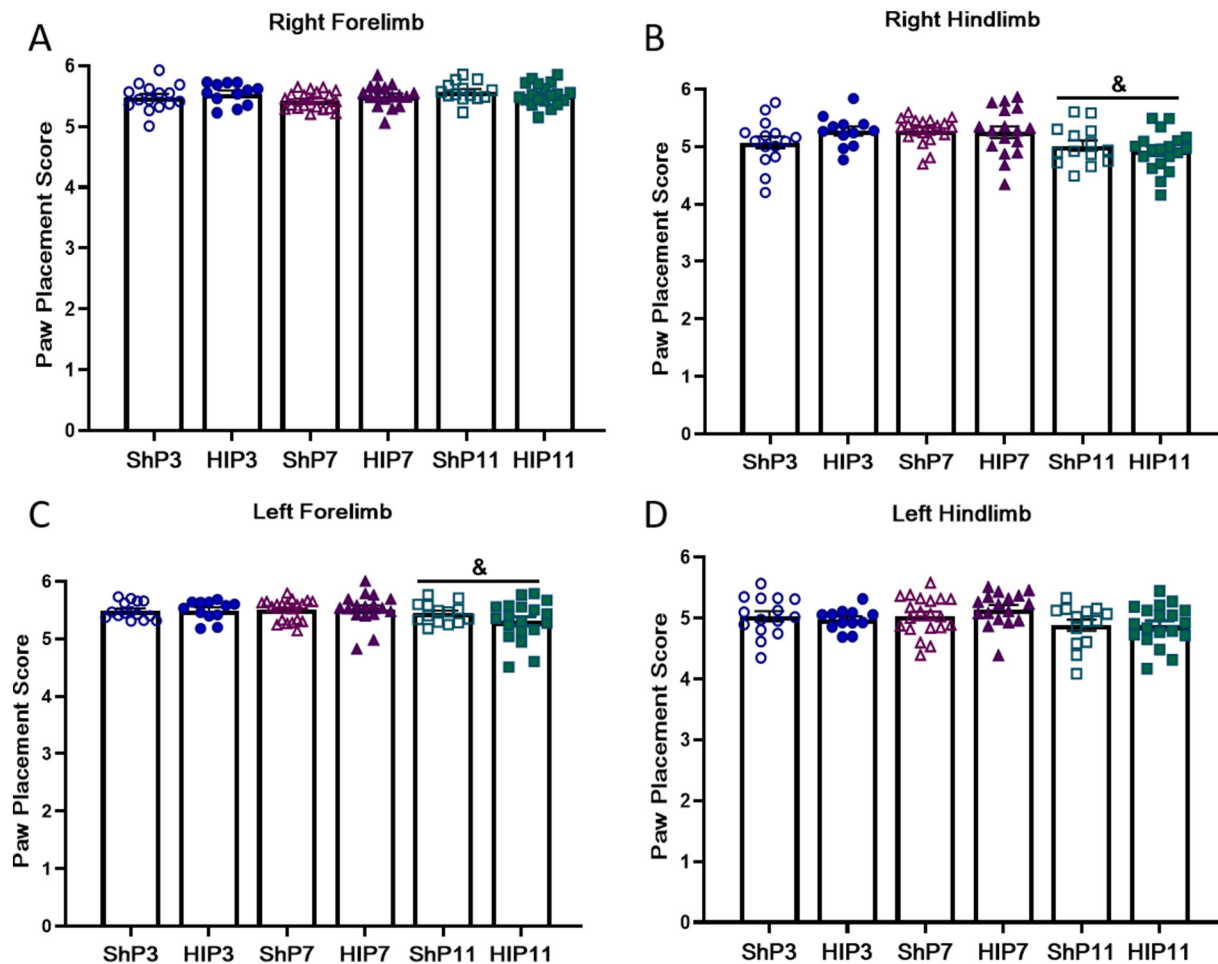


Fig. 1. Ladder walking test motor coordination assessment. Data expressed as average of Paw Placement Score  $\pm$  SE. Two-way ANOVA followed by Duncan's *post-hoc*.  $N = 14$ –18 per group. & Age effect.

manually delimited VOIs, defined on the rat templates and SUV ratio (SUVr) was calculated using the following equation  $SUVr = \text{structure SUV} / \text{Cerebellum SUV}$  (Nonose et al., 2018; Zimmer et al., 2017).

#### 2.4. $^{14}\text{C}$ -Hydroxybutyric acid and $^{14}\text{C}$ -glucose incorporation into $^{14}\text{CO}_2$

The  $^{14}\text{C}$ -BHB and  $^{14}\text{C}$ -glucose incorporation into  $^{14}\text{CO}_2$  was performed as previously described (de Assis et al., 2016; Ferreira et al., 2007; Torres et al., 2001). Briefly, animals were decapitated, the right hemisphere was quickly removed, dissected and sliced, in a process that took less than 2 min. The samples were then incubated at 37 °C for 60 min in flasks sealed with rubber caps containing 1.0 mL of HBSS (Hanks' Balanced Salt solution, pH 7.4), 0.2  $\mu\text{Ci}$  Sodium salt Beta-[1- $^{14}\text{C}$ ] hydroxybutyric acid (55 mCi/mmol, American Radiolabeled Chemicals, St. Louis, MO, EUA) and 5 mM of L-BHB sodium salt (for the  $^{14}\text{C}$ -BHB assay) or 0.1  $\mu\text{Ci}$  [U- $^{14}\text{C}$ ] glucose (55 mCi/mmol, Amersham, Little Chalfont, UK), and 5 mM of glucose (for the  $^{14}\text{C}$ -glucose assay). The gaseous phase was exchanged with a 5%  $\text{CO}_2$  and 95%  $\text{O}_2$  mixture. Small glass wells containing strips of 3 MM-Whatman paper were placed above the level of the incubation medium ( $^{14}\text{CO}_2$  wells). The assay was stopped by injecting 0.25 mL of trichloroacetic acid solution 50% (v/v) through the rubber caps, and 0.25 mL of NaOH (2.0 M) solution directly into the  $^{14}\text{CO}_2$  wells. The flasks were kept for 12 h at room temperature in order to capture  $^{14}\text{CO}_2$  into 3 MM-Whatman paper. The paper contents were transferred to vials containing a liquid scintillation mixture (toluene – Triton X<sup>®</sup>-100 (2:1, v/v); 2,5-diphenyloxazole (0.4%, v/v) and 2-*p*-phenylenebis 5-phenyloxazole (0.01%v/v), and radioactivity was measured using a liquid scintillation counter

(LKB-Wallac, Perkin Elmer, WALTHAM, MA, USA). The levels of BHB and glucose oxidation are expressed as nmol incorporated into  $\text{CO}_2/\text{g}$  of tissue /hour.

#### 2.5. Behavioral assessment

Behavioral tasks were performed between PND 60 and 80. Ladder Walking and Morris Water Maze tasks were performed for assessing animal's motor and cognitive deficits, respectively.

##### 2.5.1. Ladder walking

The motor assessment was performed using the ladder walking apparatus, which consists of two transparent acrylic walls (Diameter: 1 m. High: 20 cm) with metal rungs (Diameter: 3 mm) inserted into the walls. The ladder remained 30 cm above the ground and a dark cage was located at the end of the apparatus (Metz and Whishaw, 2002). Animals were trained for two days using a regular distance between the rungs. Along each training session, the rats walked across the ladder three times.

On the third day, the walking of the animals was evaluated using an irregular rungs pattern, *i.e.* the rungs were spaced in intervals of 1 to 3 cm. The test was video-recorded from an inferior view in order to record the four paws. The paws placement on the metal rungs were rated from 0 to 6, with zero being a total miss and six was scored for a totally correct placement (Metz and Whishaw, 2009). An error was considered when the animal slipped the paw or failed to place it on the rung. The final score corresponded to the mean of the three trials for each paw in the third day.

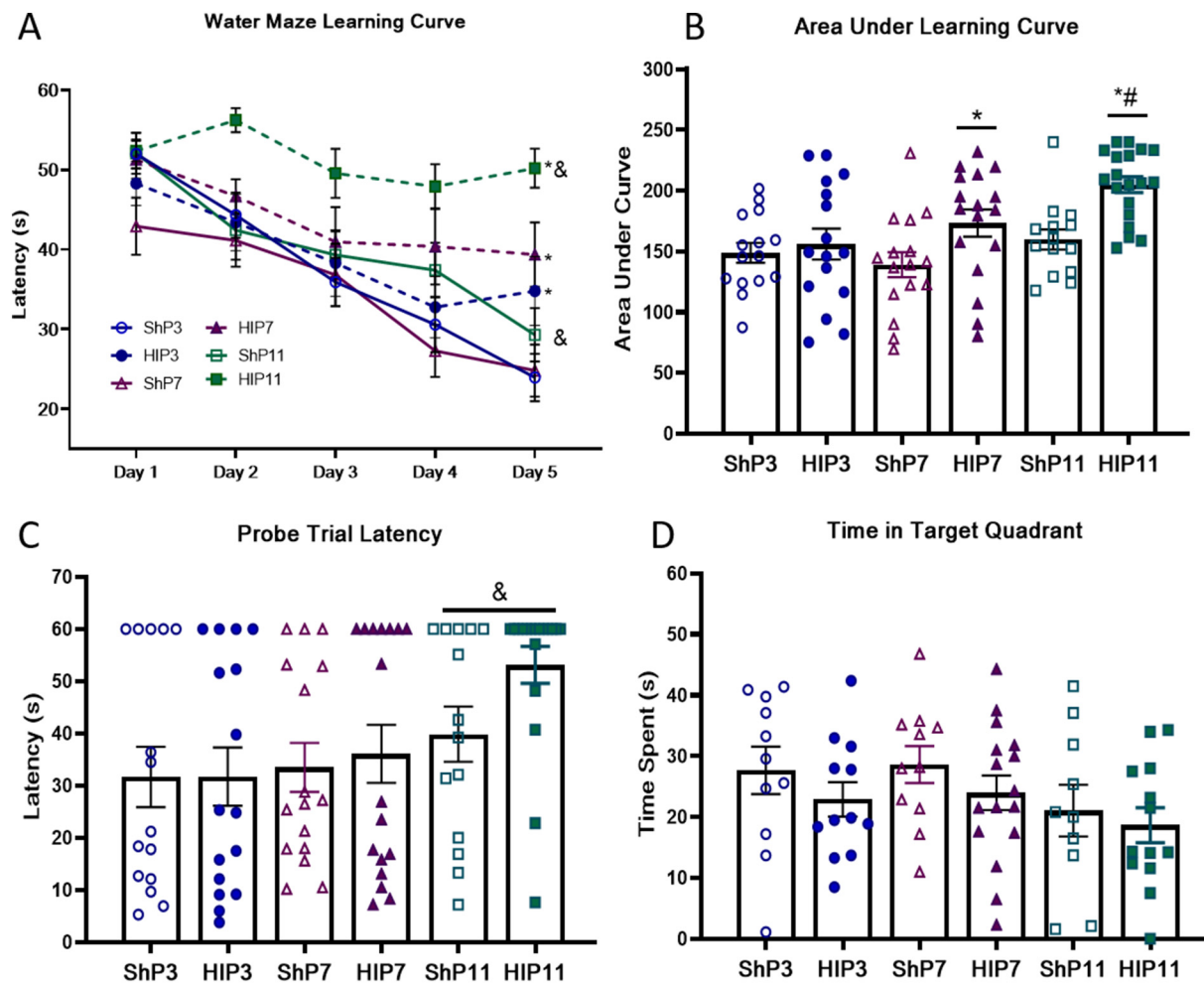


**Fig. 2.** Morris Water Maze cognitive analysis. Learning curve during the training days (A) and Area under the learning curve (B) during the five days of training. Probe trial latency to reach the platform location and (C) time spent in the target quadrant (D). Data are expressed as average ± SE. Two-way ANOVA followed by Duncan's *post-hoc*. N = 14–18 per group. \* HI vs. respective Sham; # Difference to other HI groups; & Age effect.

**Table 1**

[<sup>18</sup>F]FDG microPET imaging correlates with cognitive performance in adulthood. Pearson correlation of different brain regions with different analysis methods and the Water Maze area under curve.

Water maze	Histology		SUV 24 h		SUV 72 h	
Area under curve	(Ipsi/contralateral ratio)		(Ipsi/contralateral ratio)		(Ipsi/contralateral ratio)	
Brain region	r <sup>2</sup>	p	r <sup>2</sup>	p	r <sup>2</sup>	p
Cortex	-0.140	0.011	-0.184	0.001	-0.263	> 0.001
Striatum	-0.202	0.002	-0.111	0.009	-0.148	0.002
Hippocampus	-0.232	0.001	-0.100	0.001	-0.228	> 0.001

**Table 2**

[<sup>18</sup>F]FDG microPET imaging correlates with tissue injury observed in adulthood. Pearson correlation between histological analysis performed at adulthood and [<sup>18</sup>F]FDG microPET imaging.

Histology	SUV 24 h		SUV 72 h	
	(Ipsi/contralateral ratio)		(Ipsi/contralateral ratio)	
Brain region	r <sup>2</sup>	p	r <sup>2</sup>	p
Cortex	0.327	> 0.001	0.355	> 0.001
Striatum	0.231	0.001	0.245	0.001
Hippocampus	0.141	0.011	0.333	> 0.001

### 2.5.2. Morris water maze

Spatial memory protocol was performed as previously described (Arteni et al., 2003). Briefly, each rat performed four daily trials, during five consecutive days to find a 10 cm circumference hidden platform, which was kept in the same position during the training phase. The interval between trials was 10 min and the maximum time to find the platform was of 60 s for each animal in each attempt. If the animal was unable to find the platform it was gently placed on the platform for 15 s. The reduction in the latency to find the platform during the training days was considered an indication of learning. In the probe test, performed 24 h after the lasting training day, the platform was removed and each rat had a single 60-s trial. Latency for crossing the platform area for the first time, average speed and time spent in target quadrant

**Table 3**

[<sup>18</sup>F]FDG microPET imaging correlations with cognitive performance in adulthood separated by age. Pearson correlation of different brain regions with different analysis methods and the Water Maze area under curve. P3 = ShP3 and HIP3 groups; P7 = ShP7 and HIP7 and P11 = ShP11 and HIP11. \*Significant statistical difference.

Age	Brain region	Water maze		Histology		SUV 24 h		SUV 72 h	
		Area under curve		(Ipsi/contralateral ratio)		(Ipsi/contralateral ratio)		(Ipsi/contralateral ratio)	
		r <sup>2</sup>	p	r <sup>2</sup>	p	r <sup>2</sup>	p	r <sup>2</sup>	p
P3	Cortex	0.069	0.365	-0.005	0.766	-0.098	0.167		
	Striatum	0.107	0.253	-0.080	0.216	-0.046	0.350		
	Hippocampus	0.015	0.678	0.000	0.950	-0.013	0.628		
P7	Cortex	-0.194	0.115	-0.103	0.167	-0.040	0.409		
	Striatum	-0.315	0.037*	-0.014	0.615	-0.064	0.297		
	Hippocampus	-0.354	0.025*	-0.040	0.401	-0.065	0.292		
P11	Cortex	-0.349	0.02*	-0.501	0.001*	-0.044	0.438		
	Striatum	-0.423	0.009*	-0.328	0.013*	0.011	0.692		
	Hippocampus	-0.466	0.005*	-0.333	0.012*	-0.022	0.586		

**Table 4**

[<sup>18</sup>F]FDG microPET imaging correlating with tissue injury observed in adulthood separated by age. Pearson correlation between histological analysis performed at adulthood and [<sup>18</sup>F]FDG microPET imaging. P3 = ShP3 and HIP3 groups; P7 = ShP7 and HIP7 and P11 = ShP11 and HIP11. \*Significant statistical difference.

Age	Brain region	Histology		SUV 24 h		SUV 72 h	
		(Ipsi/contralateral ratio)		(Ipsi/contralateral ratio)		(Ipsi/contralateral ratio)	
		r <sup>2</sup>	p	r <sup>2</sup>	p	r <sup>2</sup>	p
P3	Cortex	0.510	0.004*	0.003	0.842		
	Striatum	-0.059	0.393	-0.471	0.007*		
	Hippocampus	0.410	0.014*	0.000	0.984		
P7	Cortex	-0.002	0.887	-0.154	0.185		
	Striatum	0.209	0.116	0.289	0.058		
	Hippocampus	0.282	0.062	0.001	0.908		
P11	Cortex	0.429	0.011*	0.540	0.003*		
	Striatum	0.472	0.007*	0.436	0.01*		
	Hippocampus	0.261	0.062*	0.630	0.001*		

were recorded using ANY-Maze software. The results of the probe trial were considered an indication of the animal's memory retention in the task.

## 2.6. Brain histology

Histological analysis was performed in order to assess tissue injury. In brief, animals were anesthetized (100 mg/kg of thiopental sodium, Thiopentax, Cristália®) and transcardially perfused with 0.9% saline solution and 4% paraformaldehyde solution (PFA 4%). Brains were removed from the skull and placed in 4% PFA. Then, the brains were placed in sucrose solution (30%) for cryoprotection and sliced in a cryostat (Leica) at 30 μm thickness between Bregma -1.6 and -3.8 mm (Paxinos and Watson, 2006). Every tenth section was mounted on a gelatin-coated slide and stained using hematoxylin and eosin (Sigma-Aldrich, St Louis, MO, USA). Volumes of hemisphere, cortex, striatum, corpus callosum and hippocampus were assessed using NIH-ImageJ software and calculated using Cavalieri's method, using the equation:  $\Sigma \text{area} \times (\text{interslice interval})$ . Data are expressed as volume ratio of the ipsilateral hemisphere compared to the contralateral side of carotid occlusion (Odorcyk et al., 2016).

## 2.7. Statistics

Statistical analysis was performed using SPSS-21 for Windows. Sample sizes were calculated based on previous studies using similar methodologies (Sanches et al., 2015) considering alpha = 0.05 and a power of 80%. Two-way ANOVA considering the factors I) Age (P3, P7 or P11) and II) Lesion (Sham and HI), followed by Duncan post-hoc was used in order to identify differences among the groups. In the water maze learning curve a repeated measures two-way ANOVA was performed. Data are expressed as means ± standard error. Significance was accepted whenever  $P < .05$ .

## 3. Results

### 3.1. HI did not induce significant motor impairments

In order to assess HI-induced motor impairments the ladder walking test was performed. There were no differences neither in the number of total errors, nor in the number of errors for each individual paw (data not shown). The comparison of the foot fault score showed no effect of the lesion in any of the assessed parameters. However, an effect of the age was present with a small decrease was observed in P11 groups and the in the left forelimb ( $F(5,90) = 3.89, p = .024, n = 14-18$  per group) and in the right hindlimb ( $F(5,90) = 6.11, p = .003, n = 14-18$  per group), with no differences among groups in the score of the other paws (Fig. 1A-D). The fact that there were no differences in the number of errors between HI groups and their respective Sham groups indicates that the HI insult did not induce significant motor damage, regardless of the age in which the injury occurs.

### 3.2. HI induced age-dependent cognitive deficits

The Morris water maze task was performed to assess HI-induced learning and memory impairments. During the training sessions, latency to find the platform was considered an indicative of learning. Repeated measures two-way ANOVA showed significant effect of the age and lesion ( $F(5,90) = 5.69, p = .005$  and  $F(5,90) = 15.09, p < .001$  respectively,  $n = 14-18$  per group), but no interaction ( $p = .146$ ), meaning that the HI animals had learning impairments when compared to the Sham animals and that the P11 animals also presented such impairment when compared to the other ages. In order to have an overall average for learning, the area under curve for the training days was assessed. A similar pattern was observed with differences in age and lesion ( $F(5,90) = 5.69, p = .006$  and  $F(5,90) = 15.09, p = .001$  respectively,  $n = 14-18$  per group) and no significant interaction ( $p = .156$ ). Duncan *pos-hoc* showed no difference between ShP3 and HIP3 groups, however, there was a significant learning deficit in HIP7 group compared to ShP7. Furthermore, the HIP11 group was not only different from the ShP11, but was also different from other HI groups (Fig. 2B). These results clearly show that the learning deficits are worse in animals in which HI is induced at later stages of development. The probe trial, performed 24 h after the last training session is used for assessing deficits in memory retention. There were no differences in the swimming speed (data not shown) which implies no motor deficits. The worse performance of P11 group was also present in the latency to reach the platform zone in the probe trial, where only the effect of the age was found significant ( $F(5,90) = 4.78, p = .011, n = 14-18$  per group), while the lesion ( $p = .189$ ) and the interaction ( $p = .36$ ) were not (Fig. 2C). No differences were observed in the time spent in the platform quadrant ( $F(5,90) = 1.65, p = .154, n = 14-18$  per group) (Fig. 2D). Overall, present results suggest that HI induces mainly learning deficits, and that such deficits increase when the lesion is induced at later stages of development.

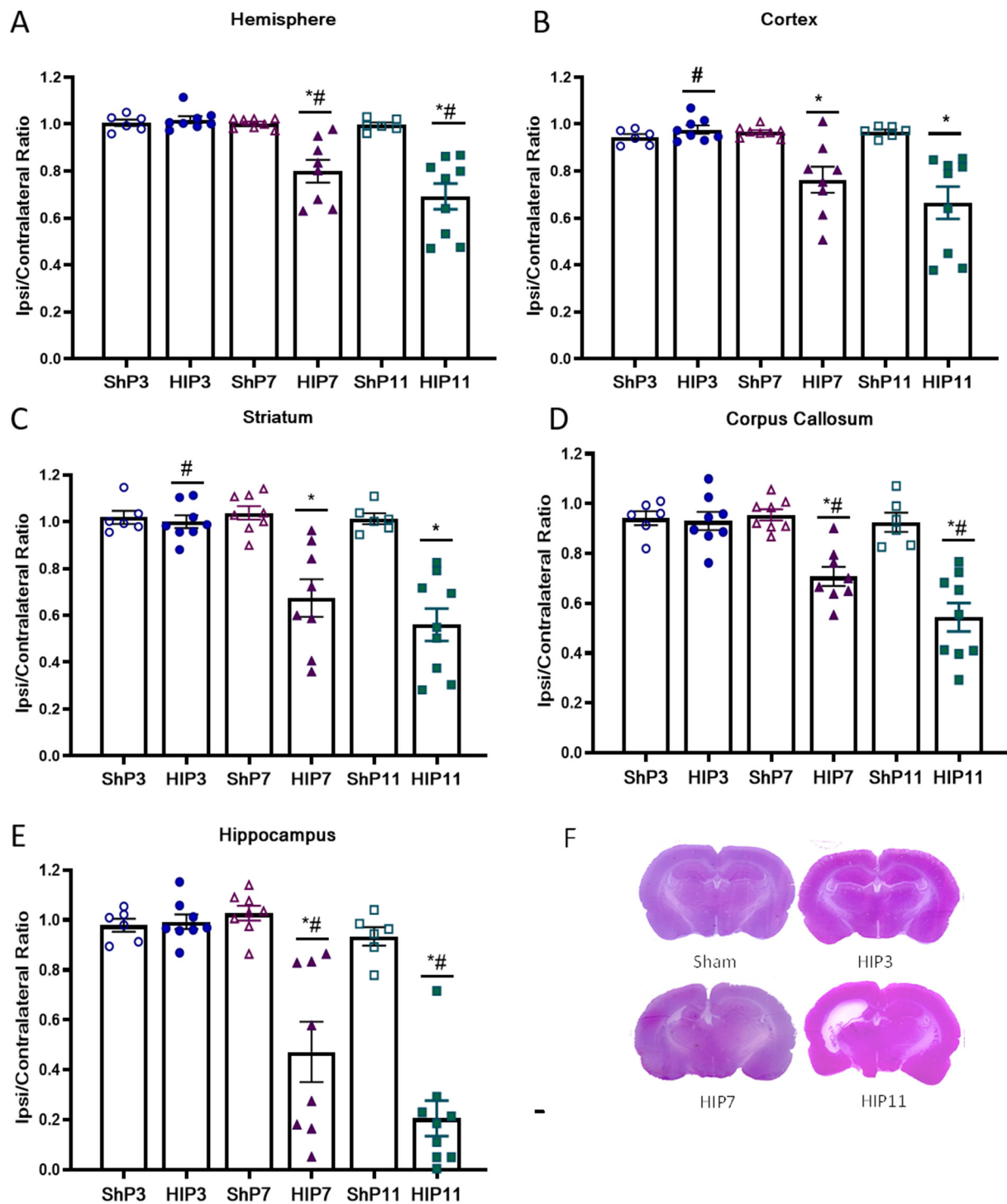


**Fig. 3.** HI-induced brain damage in different brain structures. Ipsi/contralateral volume ratio of hemispheres (A), cortices (B), striatum (C), corpus callosum (D) and hippocampi (E), as well as representative images of the HE staining (F). Data are expressed as average  $\pm$  SE. Two-way ANOVA followed by Duncan's *post-hoc*.  $N = 6-9$  per group. \* HI vs. respective Sham; # Difference to other HI groups.

### 3.3. HI induced age-dependent tissue injury

After performing behavioral tests, in order to assess HI-induced damage in motor and cognitive parameters, the volumes of main brain structures were analyzed in order to evaluate tissue injury at adulthood. The volumes of the ipsi (right) and contralateral (left) hemisphere, cortex, striatum, corpus callosum and hippocampus were analyzed and are presented as ipsi/contralateral volume ratio. The volume of all structures presented an interaction between age and lesion. Brain

hemispheres ( $F(5,40) = 11.04, p < .001, n = 6-9$  per group), corpus callosum ( $F(5,40) = 11.70, p < .001, n = 6-9$  per group) and hippocampus ( $F(5,40) = 21.22, p < .001, n = 6-9$  per group) presented the same pattern, with reductions in HIP7 and HIP11 when compared to their respective shams, with no differences between HIP3 and ShP3. In addition, the comparison among HI groups showed that the most affected group was the HIP11, which presented a greater volume loss when compared to the other HI groups, whereas the HIP7 group also presented a reduction when compared to the HIP3 group. The cortex (F

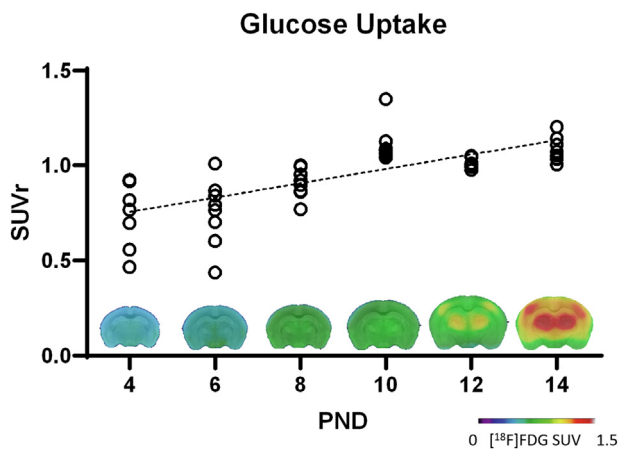


Fig. 4. Brain glucose uptake increase during neurodevelopment. Glucose Standard Uptake Value ratio (SUVr) assessed by microPET scan imaging after [ $^{18}\text{F}$ ]FDG injection in each post-natal day (PND) in non-injured rats. Linear regression ( $r^2 = 0.497$ ,  $p < .0001$ ,  $y = 0.038x + 0.604$ ,  $n = 8-10$  per group). At the graph's bottom, representative images showing SUV average for each PND (4, 6, 8, 10, 12 and 14).

(5,40) = 8.32,  $p = .001$ ,  $n = 6-9$  per group) and striatum (F(5,40) = 9.66,  $p < .001$ ,  $n = 6-9$  per group) presented a similar pattern, with HIP7 and HIP11 being different from their shams, while the HIP3 had no decrease. In these structures, however, although the HIP3 group presented less reduction in relation to other HI groups, the HIP7 and HIP11 groups were not different from each other. Altogether, these results show, in agreement with the behavioral data, that HI-induced tissue damage is more severe when induced in animals in more advanced stages of development.

### 3.4. HI induced age-dependent hypometabolism detected by microPET

After establishing the age dependent behavioral deficits and HI-induced tissue damage, the aim of this study was to assess how the injury would impact glucose brain metabolism in the first post-lesion days, namely 24 and 72 h after HI. The analysis of the standard uptake value (SUV) of the Sham groups already provides relevant information regarding the metabolic changes that the developing brain undergoes at this stage. A linear regression was performed with the SUV in the whole brain of the Sham groups showing that the glucose uptake increases linearly ( $r^2 = 0.497$ ,  $p < .0001$ ,  $y = 0.038x + 0.604$ ,  $n = 8-10$  per group) (Fig. 4). This analysis revealed a linear daily increase and that between the P4 and P14 the brain glucose uptake doubles.

The effect of HI in glucose metabolism was also assessed in different brain regions 24 and 72 h after injury, all structures presented a significant interaction between age and injury in the Two-way ANOVA test (Fig. 5). In the hippocampus at 24 h there was a reduction in the HIP11 when compared to Shp11, showing that in this region a HI-induced hypometabolism can be found at 24 h (F(5,57) = 3.68,  $p = .032$ ,  $n = 9-13$  per group). At 72 h, a similar pattern was observed with HIP11 being the only group that is different from its Sham, furthermore, HIP11 was also reduced when compared to the other HI groups (F(5,58) = 15.46,  $p < .001$ ,  $n = 9-13$  per group). The same pattern was observed in other structures, with HIP11 group presenting a reduction not only in relation to its Sham, but also from the other HI groups. This pattern was observed in the striatum (24 h: F(5,57) = 7.20,  $p = .002$ , and 72 h: F(5,58) = 3.61,  $p = .034$ ,  $n = 9-13$  per group) and cortex (24 h: F(5,57) = 8.74 and 72 h: F(5,58) = 12.55,  $p < .001$ ,  $n = 9-13$  per group) both in 24 and 72 h.

The hypometabolism in HIP11 can also be observed in Fig. 6, that shows the percentage of hypometabolism in relation to age matched Sham group. No hypometabolic areas are seen in HIP3 animals in either

24 or 72 h. In the HIP7 areas of hypometabolism can be seen only 72 h after HI, whereas in HIP11 they can be seen in both 24 and 72 h, with a greater area in comparison to the other HI groups. In agreement with behavioral and histological findings, present results also show that HI is more severe when induced in later stages of development.

### 3.5. [ $^{18}\text{F}$ ]FDG microPET metabolism in the first day post-injury correlates with cognitive and histological parameters in adulthood

Parameters that are able to predict the injury outcome are often valuable for planning the best therapeutic strategy (Negro et al., 2018). In order to assess if the [ $^{18}\text{F}$ ]FDG microPET imaging performed 24 and 72 h after HI was able to predict the cognitive deficits and size of tissue injury, bivariate correlations were performed. For assessing cognitive deficits, the main outcome was the area under curve during the water maze training phase. This parameter was compared to ipsi/contralateral ratio of histological analysis performed in adulthood and of microPET scan imaging in 3 regions of interest: Cortex, striatum, and hippocampus (Table 1).

As expected, [ $^{18}\text{F}$ ]FDG microPET imaging correlated more strongly with histological than with cognitive parameters. Interestingly, the cortex is the structure that showed the strongest correlation with an  $r^2$  of 0.355, while the striatum showed the weakest with an  $r^2$  of 0.245 in 72 h (Table 2). Again, the 72 h period presented better predictive power compared to 24 h. Overall, present results show that [ $^{18}\text{F}$ ]FDG microPET during the first post-injury days correlate with both cognitive deficits and histological damage, and that 72 h period presents better correlations to both parameters than 24 h.

When a split by age is performed, meaning doing one correlation with Shp3 and HIP3, a separate one with Shp7 and HIP7 and the same thing with the P11 groups, a different pattern emerges. In the comparison with the area under the water maze learning curve (Table 3) there are no significant correlations in the P3 groups, while in the P7 groups they were found only in histological analysis. In the P11 groups, on the other hand, there were correlations in both histology and [ $^{18}\text{F}$ ]FDG microPET at 24 h, but not at 72 h. When comparing histological data with [ $^{18}\text{F}$ ]FDG microPET (Table 4) a complex pattern emerges, with some significant correlations found in the P3 animals, while none are found in P7. Nevertheless, P11 animals showed significant correlations in all structures at both 24 h and 72 h. Overall, such results show that [ $^{18}\text{F}$ ]FDG microPET shows its highest predictive value in P11 animals, likely because of their greater lesion.

### 3.6. HI affects glucose and BHB oxidation

After observing the differences in glucose uptake using microPET scan, questions regarding the actual oxidation of such substrate and others for brain metabolism after HI remained to be answered. The first important observation was obtained assessing the Sham groups only at P4, P8 and P12. Interestingly, the  $^{14}\text{C}$ -glucose incorporation into  $^{14}\text{CO}_2$  did not present significant differences across different ages (Fig. 7), whereas  $^{14}\text{C}$ -BHB incorporation had a linear reduction of 4 fold in the same period ( $r^2 = 0.716$ ,  $p < .001$ ,  $y = -77.214x + 1044.4$ ,  $n = 6-7$  per group). These results suggest that although the uptake of glucose increases within development, the tissue capacity of oxidizing glucose remains constant. In contrast, the capacity for BHB oxidation shows greater differences within the same period in healthy animals.

Assessment using *in vivo* microPET imaging in the ipsilateral hemisphere showed no significant effects the lesion at 24 h, but showed an increase in SUVr value with age (F(5,56) = 24.46,  $p < .001$ ,  $n = 8-13$  per group), without interaction between the two factors (Fig. 8A). Furthermore, at 72 h a similar pattern is found, with significant effect only in the age (F(5,58) = 42.45,  $p < .001$ ,  $n = 8-13$  per group) no effect of the injury ( $p = .457$ ) or interaction ( $p = .122$ ). It is possible to observe that the reduction in the P3 groups was maintained, but the difference observed between P7 and P11 groups is

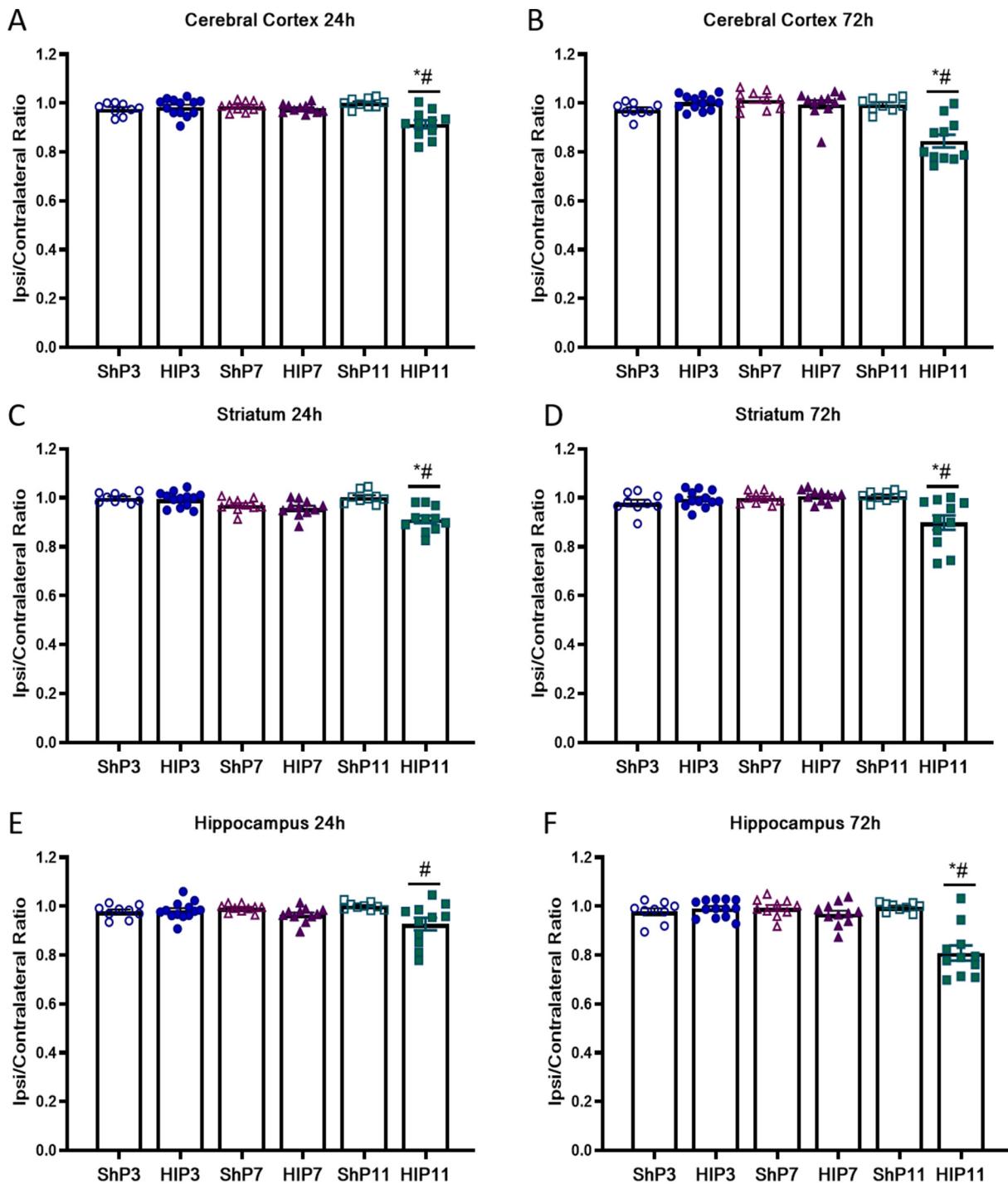


Fig. 5. HI-induced hypometabolism in different brain structures. Ipsi/contralateral SUV ratio 24 and 72 h post-HI on cortex (A, B), striatum (C, D), and hippocampus (E, F). Data expressed as average  $\pm$  SE. Two-way ANOVA followed by Duncan's *post-hoc*.  $N = 9$ –13 per group. \* HI vs. respective Sham; # Difference to other HI groups.

likely due to the effect of HI injury in the HIP11 group that reduced the average in the P11 animals in relation to the P7 ones.

In order to understand the effects of HI on substrate oxidation, the incorporation of  $^{14}\text{C}$ -Glucose and  $^{14}\text{C}$ -BHB were assessed in the right hemisphere at 24 and 72 h after HI.  $^{14}\text{C}$ -Glucose incorporation into  $^{14}\text{CO}_2$  assessed 24 h after HI showed an interaction between age and lesion ( $F(5,41) = 4.16, p = .023, n = 6$ –10 per group). A reduction in both HIP7 and HIP11 was observed when compared to their respective Shams, whereas the HIP3 group did not (Fig. 8C). A similar pattern was observed at 72 h, also presenting an interaction between the age and

lesion ( $F(5,39) = 6.38, p = .004, n = 7$ –8 per group), although only the HIP11 group presented a reduction when compared to its respective Sham difference (Fig. 8D). These results show that HI is able to induce a reduction in the brain's capacity to use glucose as an energy substrate in an age-dependent manner, once again, with animals in which injury was induced in latter stages of development presenting more detrimental effects.

Another important substrate for brain metabolism is BHB, mainly in the early stages of CNS development. Here, the  $^{14}\text{C}$ -BHB incorporation into  $^{14}\text{CO}_2$  assessed 24 h after HI revealed an effect of age (F

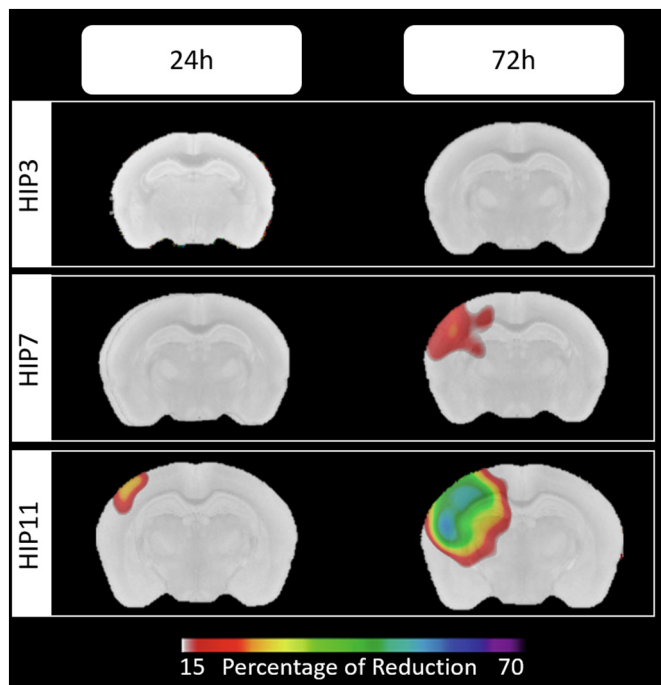


**Fig. 6.** Hypometabolism decrease percentage following HI. Images showing areas with 15% or more of hypometabolism after HI induced at the three different ages and assessed 24 and 72 h after injury compared to their respective Sham group. An increase in the hypometabolic area can be seen when HI is induced in latter stages of development. It is also possible to notice that this area grows from 24 to 72 h after the initial insult.

(5,41) = 46.47,  $p < .001$ ,  $n = 7-8$  per group), but not of the lesion ( $p = .073$ ), with significant differences between all ages, with P3 animals presenting the highest levels (Fig. 8E). However, it is worth noticing a great tendency of reduction between the ShP3 and HIP3 animals only. A similar pattern was observed in 72 h, with the only significant effect being the age ( $F(5,40) = 3.98$ ,  $p = .026$ ,  $n = 6-11$  per group), with the P3 group being different from the P11 group, but presenting no differences in relation to the P7 group. Here, it should also be observed that the HIP3 presents higher levels in relation to its sham, in contrast to the patterns observed at 24 h (Fig. 8F). These results show that HI alters glucose consumption in HIP7 and even more in the HIP11 groups, whereas in the HIP3 group BHB seems to more affected.

#### 4. Discussion

Present study investigated the different responses to neonatal HI injury induced in different neurodevelopmental stages. The injury showed to be more severe when induced in later stages (causing more cognitive deficits, tissue damage and hypometabolism assessed through microPET imaging in the early post-injury days). Differences in brain metabolism that occur at this age seem to play a pivotal role, namely the more prevalent usage of BHB as a metabolic substrate in earlier stages of development compared to glucose. In addition, microPET imaging data, mainly 72 h after the neonatal insult, showed significant correlations with behavioral and histological parameters observed at adulthood, showing to be a potential tool to predict the long-term outcome induced by HI. Overall, present results show that brain metabolism plays a pivotal role in the different outcomes observed in HI induced in different stages of development and suggest that these factors present promising clinical value, being as predictors of the injury outcome or as therapeutic targets.

No significant motor impairments were observed in any of the experimental groups with the injury protocol used in this study, confirming previous literature (Greggio et al., 2014; Miguel et al., 2015; Odorcyk et al., 2016; Sanches et al., 2019). Nevertheless, HI cognitive deficits were clear, being more severe when the injury was induced in more advanced stages of development (Fig. 2). Previous studies have investigated the different behavioral outcomes in animals exposed to the same HI model at P3 and P7 (Alexander et al., 2014; Sanches et al., 2015) found similar results, with P7 animals being more affected than P3. In the present study P11 animals were also included, since they resemble the term infant more closely than the P7 animals (Patel et al., 2014, 2015). Indeed, an interesting pattern emerged from these experiments, with P3 animals presenting almost no damage, while increased damage was observed in P7 animals and P11 animals were the most affected. The same pattern was present in histological analysis of the volume of brain structures, namely the cortex, striatum, corpus callosum and hippocampus (Fig. 3). These results are again in accordance to previous studies comparing differences between P3 and P7 animals (Alexander et al., 2014; Sanches et al., 2015).

The degree of HI damage is greatly dependent on brain metabolism and it is well documented that it presents significant changes during development (Brekke et al., 2015). Indeed, in the present study, a linear increase in the glucose uptake in the brain was observed between P4 and P14, assessed by microPET scan imaging *in vivo*, (Fig. 4). Such findings are in accordance with previous studies that, using different methodologies, found an increase in glucose utilization in the brain is expected during early development (Brekke et al., 2017). Nevertheless, glucose oxidation assay showed a different pattern, with no differences among the Sham groups, but with more glucose oxidation in the HIP3

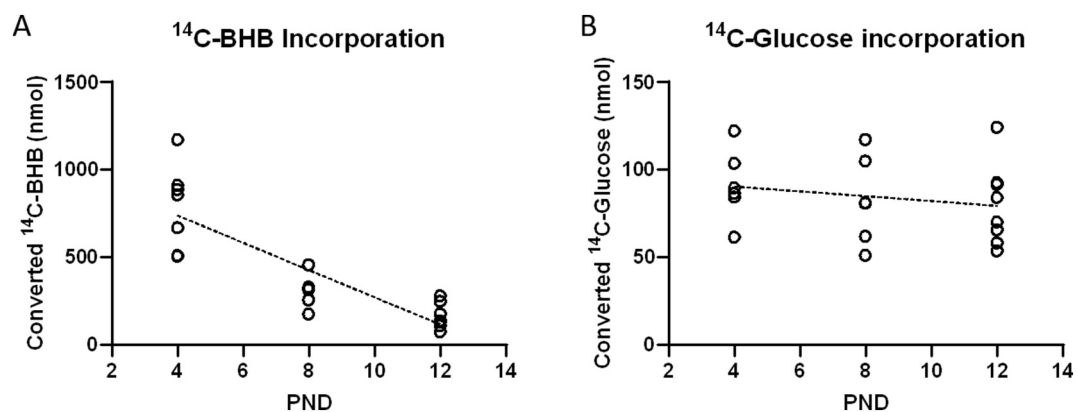


**Fig. 7.** Beta-hydroxybutyrate (BHB) oxidation capacity in the total brain tissue. With the increase in age, while with glucose it remains unchanged.  $^{14}\text{C}$ -BHB incorporation into  $^{14}\text{CO}_2$  reduces linearly within the assessed post-natal days (PND) (A) ( $r^2 = 0.716$ ,  $p < .001$ ,  $y = -77.214x + 1044.4$ ). Whereas  $^{14}\text{C}$ -Glucose incorporation into  $^{14}\text{CO}_2$  remained unchanged.  $N = 6-7$  per group.

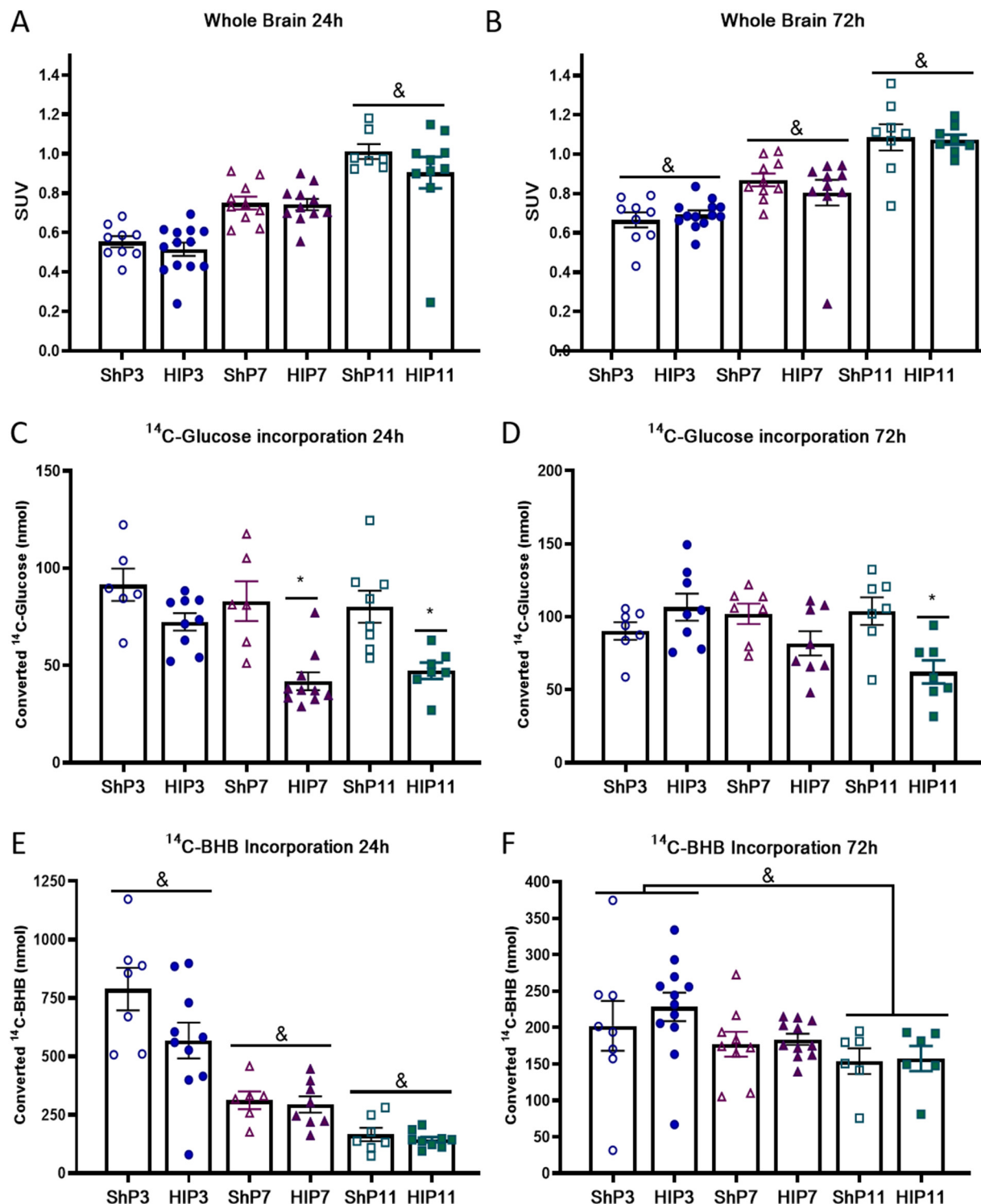


**Fig. 8.** HI-induced age-dependent metabolic substrate utilization changes in both *in vivo* and *ex vivo* in the ipsilateral hemisphere. *In vivo* assessment of glucose uptake 24 h (A) and 72 h (B) after HI by microPET scan imaging after [<sup>18</sup>F]FDG injection (N = 8–13 per group). *Ex vivo* evaluation of <sup>14</sup>C-Glucose incorporation into <sup>14</sup>CO<sub>2</sub> (C and D) and of <sup>14</sup>C-BHB incorporation into <sup>14</sup>CO<sub>2</sub> (E and F) (N = 6–11 per group). Data are expressed as average ± SE. Two-way ANOVA followed by Duncan's *post-hoc*. \* HI vs. respective Sham; # Difference to the other groups; & Age effect.

animals (Figs. 8C). These differences occur because the main limiting factor for glucose uptake in the brain is the small amount of glucose transporters present in the blood-brain barrier (Brekke et al., 2015; Vannucci et al., 1994), whereas <sup>14</sup>C-glucose incorporation into <sup>14</sup>CO<sub>2</sub> assay assesses the capacity of cells to oxidize it *ex vivo*, without the limitation imposed by glucose transporters. Altogether, results presented here suggest that one of the mechanisms that can explain the P3

intrinsic neuroprotection is the resilience of the systems involved in the glucose oxidation system, since it was the only age in which <sup>14</sup>C-glucose incorporation into <sup>14</sup>CO<sub>2</sub> was not reduced by HI injury.

During the neonatal period, brain utilization of ketone bodies such as BHB is increased in comparison to the adult brain (Brekke et al., 2017). In our study, the brain capacity of oxidizing BHB is at least 4 times greater in the P4 brain when compared to the P12 (Fig. 7A). This

increased capacity of utilizing BHB, associated to the unchanged glucose usage as energetic source is likely to be involved in the P3 brain intrinsic protection to HI insult. Present results also show a relevant pattern in the BHB oxidation capacity in which P3 animals show increased capacity of BHB oxidation in relation to the other ages, which are probably underlying the resilience of the more immature brain to HI injury. Interestingly, the protective effects of BHB have been previously demonstrated in a study that administered exogenous BHB after HI and showed a reduction of lesion size and cell death (Lee et al., 2018). It has also been demonstrated that the positive effects of dexamethasone treatment are likely dependent on an increase in BHB levels in the blood (Dardzinski et al., 2000). Interestingly, the ketogenic diet is an efficient and safe therapeutic approach for pediatric refractory epilepsy (Cai et al., 2017; Neal et al., 2009), suggesting that BHB administration, as well as ketogenic diet, have high translational value. Overall, present results show that the higher utilization of BHB is involved in the reduced lesion observed in animals in earlier stages of development, making it a promising therapeutic target that ought to be further investigated.

Furthermore, microPET [<sup>18</sup>F]FDG has provided important insights in the HI pathophysiology. To the best of our knowledge, this is the first study that has used this method to assess the neonatal brain after HI injury in rodents. Here, we show that HIP11 group presented a significant glucose hypometabolism, whereas no significant differences were observed in the HIP7 or HIP3 groups (Fig. 5). The hypometabolism mentioned here should be interpreted with caution, since cell death, oxidative stress and inflammation are occurring at this period, which leads to edema and liquification of the brain tissue. This means that the reduction of glucose uptake should not be understood as a simple reduction of cellular metabolism, but as a marker of brain damage. In agreement with findings obtained in clinical studies (Shi et al., 2012; Thorngren-Jerneck et al., 2001), here, stronger correlations were observed between adult cognitive deficits and microPET [<sup>18</sup>F]FDG 72 h post-injury compared to those based on adult histology when all groups were included (Table 1). Although it is likely that an analysis of volume of brain structures performed in the same time points as the microPET [<sup>18</sup>F]FDG imaging would reveal more powerful correlations, we aimed to assess its ability to predict the resulting histological lesion in the adult, therefore, histological analysis was performed only at adulthood. Indeed, all structures assessed, namely the cortex, striatum and hippocampus presented significant correlations. However, the striatum parameters presented the weakest whereas the cortex presented the strongest predictive value. When the correlations are splitted by age, as shown in Tables 3 and 4, it is possible to see that P11 animals present the correlations with higher predictive value. This is likely due to the more severe injury presented by animals of this age that translates in higher cognitive deficits, tissue damage and hypometabolism. Previous studies have correlated [<sup>18</sup>F]FDG microPET to behavioral assessments in a model of epilepsy induced by pilocarpine injection, showing significant correlations between behavioral parameters, such as social interactions and anxiety tests and imaging (Di Liberto et al., 2018; van Dijk et al., 2018; Zanirati et al., 2018). A recent study from our research group showed correlations between histological and behavioral tasks of PET scan analysis performed in adulthood in a model of HI induced at P7 (Nunes Azevedo et al., 2020). Nevertheless, the comparison between the predictive values of the present study and the previously mentioned ones is limited by the experimental model, different behavioral tasks used, as well as different statistical analysis and more importantly, because both behavioral tasks and microPET [<sup>18</sup>F]FDG were performed during adulthood (usually with few days of difference between the imaging acquisition and behavioral tasks).

Although results are interesting and confirm the working hypothesis, there are a few limitations in the present study. The use of male animals only leaves possible sex-differences unexplored and it is known that response to HI injury and to several treatments are sex-specific (Netto et al., 2017). Limitations intrinsic to the animal model are also

present; here it is shown that the immature rat brain is less susceptible to HI injury, while in humans it is known that prematurity worsens the prognosis of affected newborns (Volpe, 2009). Therefore, present results ought to be interpreted with caution.

Overall, present study has shown that P3 brain has an intrinsic neuroprotection, showing less or no effects of HI-induced injury in behavioral and histological parameters. This phenomenon can be explained, at least in part, by a more resilient capacity of oxidizing glucose and mainly by a greater capacity of using BHB as an alternative metabolic substrate. MicroPET scan analysis in the first post-injury days presented significant correlations to behavioral deficits and tissue injury observed in adulthood, suggesting that it should be helpful in clinical settings. Present results suggest that brain metabolism and mainly BHB seem to be promising therapeutic strategies for the treatment of neonatal hypoxia ischemia, such parameters are involved in the greater resistance of neonatal brain to metabolic challenges.

## Acknowledgements

This study was supported by research grants from the Conselho Nacional de Desenvolvimento Científico e Tecnológico (CNPq, Brazil; Chamada Universal MCTI/CNPq No 01/2016, grant number 405470/2016-9) and PUCRS. E. R. Zimmer, C A Netto, and J.C. DaCosta are CNPq researchers.

## References

- Alexander, M., Garbus, H., Smith, A.L., Rosenkrantz, T.S., Fitch, R.H., 2014. Behavioral and histological outcomes following neonatal HI injury in a preterm (P3) and term (P7) rodent model. *Behav. Brain Res.* 259, 85–96. <https://doi.org/10.1016/j.bbr.2013.10.038>.
- Arteni, N.S., Salgueiro, J., Torres, I., Achaval, M., Netto, C.A., 2003. Neonatal cerebral hypoxia-ischemia causes lateralized memory impairments in the adult rat. *Brain Res.* 973, 171–178. [https://doi.org/10.1016/S0006-8993\(03\)02436-3](https://doi.org/10.1016/S0006-8993(03)02436-3).
- Brekke, E., Morken, T.S., Sonnewald, U., 2015. Glucose metabolism and astrocyte-neuron interactions in the neonatal brain. *Neurochem. Int.* 82, 33–41. <https://doi.org/10.1016/j.neuint.2015.02.002>.
- Brekke, E., Berger, H.R., Widerøe, M., Sonnewald, U., Morken, T.S., 2017. Glucose and intermediary metabolism and astrocyte-neuron interactions following neonatal hypoxia-ischemia in rat. *Neurochem. Res.* 42, 115–132. <https://doi.org/10.1007/s11064-016-2149-9>.
- Cai, Q.Y., Zhou, Z.J., Luo, R., Gan, J., Li, S.P., Mu, D.Z., Wan, C.M., 2017. Safety and tolerability of the ketogenic diet used for the treatment of refractory childhood epilepsy: a systematic review of published prospective studies. *World J. Pediatr.* <https://doi.org/10.1007/s12519-017-0053-2>.
- Calabrese, E., Badea, A., Watson, C., Johnson, G.A., 2013. A quantitative magnetic resonance histology atlas of postnatal rat brain development with regional estimates of growth and variability. *Neuroimage.* <https://doi.org/10.1016/j.neuroimage.2013.01.017>.
- Chiang, M.C., Jong, Y.J., Lin, C.H., 2017. Therapeutic hypothermia for neonates with hypoxic ischemic encephalopathy. *Pediatr. Neonatol.* <https://doi.org/10.1016/j.pedneo.2016.11.001>.
- Dagnino, A.P.A., Da Silva, R.B.M., Chagastelles, P.C., Pereira, T.C.B., Venturin, G.T., Greggio, S., Da Costa, J.C., Bogo, M.R., Campos, M.M., 2019. Nociceptin/orphanin FQ receptor modulates painful and fatigue symptoms in a mouse model of fibromyalgia. *Pain* 160, 1383–1401. <https://doi.org/10.1097/j.pain.0000000000001513>.
- Dardzinski, B.J., Smith, S.L., Towfighi, J., Williams, G.D., Vannucci, R.C., Smith, M.B., 2000. Increased plasma beta-hydroxybutyrate, preserved cerebral energy metabolism, and amelioration of brain damage during neonatal hypoxia ischemia with dexamethasone pretreatment. *Pediatr. Res.* <https://doi.org/10.1203/00006450-200008000-00021>.
- de Assis, A.M., da Silva, J.S., Rech, A., Longoni, A., Nonose, Y., Repond, C., de Bittencourt Pasquali, M.A., Moreira, J.C.F., Souza, D.O., Pellerin, L., 2016. Cerebral ketone body oxidation is facilitated by a high fat diet enriched with advanced glycation end products in normal and diabetic rats. *Front. Neurosci.* <https://doi.org/10.3389/fnins.2016.00509>.
- Di Liberto, V., van Dijk, R.M., Brendel, M., Waldron, A.M., Möller, C., Koska, I., Seiffert, I., Gualtieri, F., Gildehaus, F.J., von Ungern-Sternberg, B., Lindner, M., Ziegler, S., Palme, R., Hellweg, R., Gass, P., Bartenstein, P., Potschka, H., 2018. Imaging correlates of behavioral impairments: an experimental PET study in the rat pilocarpine epilepsy model. *Neurobiol. Dis.* <https://doi.org/10.1016/j.nbd.2018.06.010>.
- Ferreira, G.C., Tonin, A., Schuck, P.F., Viegas, C.M., Ceoloto, P.C., Latini, A., Perry, M.L.S., Wyse, A.T.S., Dutra-Filho, C.S., Wannmacher, C.M.D., Vargas, C.R., Wajner, M., 2007. Evidence for a synergistic action of glutaric and 3-hydroxyglutaric acids disturbing rat brain energy metabolism. *Int. J. Dev. Neurosci.* <https://doi.org/10.1016/j.ijdevneu.2007.05.009>.

- Greggio, S., De Paula, S., Azevedo, P.N., Venturin, G.T., Dacosta, J.C., 2014. Intra-arterial transplantation of human umbilical cord blood mononuclear cells in neonatal hypoxic-ischemic rats. *Life Sci.* <https://doi.org/10.1016/j.lfs.2013.10.017>.
- Jacobs, S.E., Berg, M., Hunt, R., Tarnow-Mordi, W.O., Inder, T.E., Davis, P.G., 2013. Cooling for newborns with hypoxic ischaemic encephalopathy. *Cochrane Database Syst. Rev.* <https://doi.org/10.1002/14651858.CD003311.pub3>.
- Lee, B.S., Woo, D.C., Woo, C.W., Kim, K.S., 2018. Exogenous  $\beta$ -Hydroxybutyrate treatment and Neuroprotection in a suckling rat model of hypoxic-ischemic encephalopathy. *Dev. Neurosci.* <https://doi.org/10.1159/000486411>.
- Metz, G.A., Whishaw, I.Q., 2002. Cortical and subcortical lesions impair skilled walking in the ladder rung walking test: a new task to evaluate fore- and hindlimb stepping, placing, and co-ordination. *J. Neurosci. Methods.* [https://doi.org/10.1016/S0165-0270\(02\)00012-2](https://doi.org/10.1016/S0165-0270(02)00012-2).
- Metz, G.A., Whishaw, I.Q., 2009. The ladder rung walking task: a scoring system and its practical application. *J. Vis. Exp.* <https://doi.org/10.3791/1204>.
- Miguel, P.M., Schuch, C.P., Rojas, J.J., Carletti, J.V., Deckmann, I., Martinato, L.H.M., Pires, A.V., Bizarro, L., Pereira, L.O., 2015. Neonatal hypoxia-ischemia induces attention-deficit hyperactivity disorder-like behavior in rats. *Behav. Neurosci.* 129, 309–320.
- Neal, E.G., Chaffe, H., Schwartz, R.H., Lawson, M.S., Edwards, N., Fitzsimmons, G., Whitney, A., Cross, J.H., 2009. A randomized trial of classical and medium-chain triglyceride ketogenic diets in the treatment of childhood epilepsy. *Epilepsia.* <https://doi.org/10.1111/j.1528-1167.2008.01870.x>.
- Negro, S., Benders, M.J.N.L., Tataranno, M.L., Coviello, C., De Vries, L.S., Van Bel, F., Groenendaal, F., Longini, M., Proietti, F., Belvisi, E., Buonocore, G., Perrone, S., 2018. Early prediction of hypoxic-ischemic brain injury by a new panel of biomarkers in a population of term newborns. *Oxidative Med. Cell. Longev.* <https://doi.org/10.1155/2018/7608108>.
- Netto, C.A., Sanches, E., Odorcyk, F.K., Duran-Carabali, L.E., Weis, S.N., 2017. Sex-dependent consequences of neonatal brain hypoxia-ischemia in the rat. *J. Neurosci. Res.* <https://doi.org/10.1002/jnr.23828>.
- Nonose, Y., Gewehr, P.E., Almeida, R.F., da Silva, J.S., Bellaver, B., Martins, L.A.M., Zimmer, E.R., Greggio, S., Venturin, G.T., Da Costa, J.C., Quincozes-Santos, A., Pellerin, L., de Souza, D.O., de Assis, A.M., 2018. Cortical bilateral adaptations in rats submitted to focal cerebral ischemia: emphasis on glial metabolism. *Mol. Neurobiol.* <https://doi.org/10.1007/s12035-017-0458-x>.
- Nunes Azevedo, P., Zanirati, G., Teribele Venturin, G., Garcia Schu, G., Elena Durán-Carabali, L., Kawa Odorcyk, F., Vinicius Soares, A., de Oliveira Laguna, G., Alexandre Netto, C., Rigon Zimmer, E., Costa da Costa, J., Greggio, S., 2020. Long-term changes in metabolic brain network drive memory impairments in rats following neonatal hypoxia-ischemia. *Neurobiol. Learn. Mem.* <https://doi.org/10.1016/j.nlm.2020.107207>.
- Odorcyk, F.K., Sanches, E.F., Nicola, F.C., Moraes, J., Pettenuzzo, L.F., Kolling, J., Siebert, C., Longoni, A., Konrath, E.L., Wyse, A., Netto, C.A., 2016. Administration of Huperzia quadrifariata extract, a cholinesterase inhibitory alkaloid mixture, has neuroprotective effects in a rat model of cerebral hypoxia-ischemia. *Neurochem. Res.* 42, 552–562. <https://doi.org/10.1007/s11064-016-2107-6>.
- Parent, M.J., Zimmer, E.R., Shin, M., Kang, M.S., Fonov, V.S., Mathieu, A., Aliaga, A., Kostikov, A., do Carmo, S., Dea, D., Poirier, J., Soucy, J.P., Gauthier, S., Cuello, A.C., Rosa-Neto, P., 2017. Multimodal imaging in rat model recapitulates Alzheimer's disease biomarkers abnormalities. *J. Neurosci.* <https://doi.org/10.1523/JNEUROSCI.1346-17.2017>.
- Park, W.S., Chang, Y.S., Lee, M., 2001. Effects of hyperglycemia or hypoglycemia on brain cell membrane function and energy metabolism during the immediate reoxygenation-reperfusion period after acute transient global hypoxia-ischemia in the newborn piglet. *Brain Res.* [https://doi.org/10.1016/S0006-8993\(01\)02295-8](https://doi.org/10.1016/S0006-8993(01)02295-8).
- Patel, S.D., Pierce, L., Ciardiello, A.J., Vannucci, S.J., 2014. Neonatal encephalopathy: pre-clinical studies in neuroprotection. *Biochem. Soc. Trans.* 42, 564–568. <https://doi.org/10.1042/BST20130247>.
- Patel, S.D., Pierce, L., Ciardiello, A., Hutton, A., Paskewitz, S., Aronowitz, E., Voss, H.U., Moore, H., Vannucci, S.J., 2015. Therapeutic hypothermia and hypoxia-ischemia in the term-equivalent neonatal rat: characterization of a translational preclinical model. *Pediatr. Res.* 78, 264–271. <https://doi.org/10.1038/pr.2015.100>.
- Paxinos, G., Watson, C., 2006. *The Rat Brain in Stereotaxic Coordinates*, Sixth ed. 170. Acad. Press, pp. 547612. [https://doi.org/10.1016/0143-4179\(83\)90049-5](https://doi.org/10.1016/0143-4179(83)90049-5).
- Perlman, J.M., 2004. Brain injury in the term infant. *Semin. Perinatol.* 28, 415–424. <https://doi.org/10.1053/j.semper.2004.10.003>.
- Pinchefskey, E.F., Hahn, C.D., Kamino, D., Chau, V., Brant, R., Moore, A.M., Tam, E.W.Y., 2019. Hyperglycemia and glucose variability are associated with worse brain function and seizures in neonatal encephalopathy: a prospective cohort study. *J. Pediatr.* <https://doi.org/10.1016/j.jpeds.2019.02.027>.
- Sanches, E.F., Arteni, N.S., Nicola, F., Boisserand, L., Willborn, S., Netto, C.A., 2013. Early hypoxia-ischemia causes hemisphere and sex-dependent cognitive impairment and histological damage. *Neuroscience* 237, 208–215. <https://doi.org/10.1016/j.neuroscience.2013.01.066>.
- Sanches, E.F., Arteni, N., Nicola, F., Aristimunha, D., Netto, C.A., 2015. Sexual dimorphism and brain lateralization impact behavioral and histological outcomes following hypoxia-ischemia in P3 and P7 rats. *Neuroscience* 290, 581–593. <https://doi.org/10.1016/j.neuroscience.2014.12.074>.
- Sanches, E.F., van de Looij, Y., Toulotte, A., Sizonenko, S.V., Lei, H., 2019. Mild neonatal brain hypoxia-ischemia in very immature rats causes long-term behavioral and cerebellar abnormalities at adulthood. *Front. Physiol.* <https://doi.org/10.3389/fphys.2019.00634>.
- Semple, B.D., Blomgren, K., Gimlin, K., Ferriero, D.M., Noble-Haeusslein, L.J., 2013. Brain development in rodents and humans: identifying benchmarks of maturation and vulnerability to injury across species. *Prog. Neurobiol.* 106–107, 1–16. <https://doi.org/10.1016/j.pneurobio.2013.04.001>.
- Shi, Y., Zhao, J.N., Liu, L., Hu, Z.X., Tang, S.F., Chen, L., Jin, R. Bin, 2012. Changes of positron emission tomography in newborn infants at different gestational ages, and neonatal hypoxic-ischemic encephalopathy. *Pediatr. Neurol.* <https://doi.org/10.1016/j.pediatrneurol.2011.11.005>.
- Sizonenko, S.V., Kiss, J.Z., Inder, T., Gluckman, P.D., Williams, C.E., 2005. Distinctive neuropathologic alterations in the deep layers of the parietal cortex after moderate ischemic-hypoxic injury in the P3 immature rat brain. *Pediatr. Res.* 57, 865–872. <https://doi.org/10.1203/01.PDR.0000157673.36848.67>.
- Thorngren-Jerneck, K., Ohlsson, T., Sandell, A., Erlandsson, K., Strand, S.E., Ryding, E., Svenningsen, N.W., 2001. Cerebral glucose metabolism measured by positron emission tomography in term newborn infants with hypoxic ischemic encephalopathy. *Pediatr. Res.* <https://doi.org/10.1203/00006450-200104000-00010>.
- Torres, I.L.S., Gamaro, G.D., Silveira-Cucco, S.N., Michalowski, M.B., Corrêa, J.B., Perry, M.L.S., Dalmaz, C., 2001. Effect of acute and repeated restraint stress on glucose oxidation to CO<sub>2</sub> in hippocampal and cerebral cortex slices. *Braz. J. Med. Biol. Res.* <https://doi.org/10.1590/S0100-879X2001000100013>.
- van Dijk, R.M., Di Liberto, V., Brendel, M., Waldron, A.M., Möller, C., Gildehaus, F.J., von Ungern-Sternberg, B., Lindner, M., Ziegler, S., Hellweg, R., Gass, P., Bartenstein, P., Potschka, H., 2018. Imaging biomarkers of behavioral impairments: a pilot micro-positron emission tomographic study in a rat electrical post-status epilepticus model. *Epilepsia.* <https://doi.org/10.1111/epi.14586>.
- Vannucci, S.J., Seaman, L.B., Brucklacher, R.M., Vannucci, R.C., 1994. Glucose transport in developing rat brain: glucose transporter proteins, rate constants and cerebral glucose utilization. *Mol. Cell. Biochem.* <https://doi.org/10.1007/BF00926756>.
- Volpe, J.J., 2009. Brain injury in premature infants: a complex amalgam of destructive and developmental disturbances. *Lancet Neurol.* [https://doi.org/10.1016/S1474-4422\(08\)70294-1](https://doi.org/10.1016/S1474-4422(08)70294-1).
- Zanirati, G., Azevedo, P.N., Venturin, G.T., Greggio, S., Alcará, A.M., Zimmer, E.R., Feltes, P.K., DaCosta, J.C., 2018. Depression comorbidity in epileptic rats is related to brain glucose hypometabolism and hypersynchronicity in the metabolic network architecture. *Epilepsia.* <https://doi.org/10.1111/epi.14057>.
- Zimmer, E.R., Parent, M.J., Souza, D.G., Leuzy, A., Lecrux, C., Kim, H.I., Gauthier, S., Pellerin, L., Hamel, E., Rosa-Neto, P., 2017. [18F]FDG PET signal is driven by astroglial glutamate transport. *Nat. Neurosci.* <https://doi.org/10.1038/nn.4492>.
- Zou, R., Xiong, T., Zhang, L., Li, S., Zhao, F., Tong, Y., Qu, Y., Mu, D., 2018. Proton magnetic resonance spectroscopy biomarkers in neonates with hypoxic-ischemic encephalopathy: a systematic review and meta-analysis. *Front. Neurol.* <https://doi.org/10.3389/fneur.2018.00732>.